Analytical and Bioanalytical Chemistry (2022) 414:1899–1907
https://doi.org/10.1007/s00216-021-03825-3

RESEARCH PAPER

A low-noise ratiometric fluorescence biosensor for detection of Pb^{2+} based on DNAzyme and exonuclease III–assisted cascade signal amplification

Huali Jin[1] · Ruike Liu[1] · Tian Bai[2] · Min Wei[1] · Baoshan He[1] · Zhiguang Suo[1]

Received: 20 October 2021 / Revised: 24 November 2021 / Accepted: 1 December 2021 / Published online: 7 January 2022

Abstract

As a common heavy metal ion with strong toxicity and wide distribution, lead ions (Pb^{2+}) had great harm to the human body. In this work, a low-noise ratiometric fluorescence biosensor was developed based on Pb^{2+}-dependent DNAzyme and exonuclease III (Exo III)–assisted cascade signal amplification. Firstly, the substrate chain of DNAzyme (S-DNA) was modified on the surface of magnetic beads (MBs) through the combination of biotin and streptavidin, and then the enzyme chain of DNAzyme (E-DNA) was connected to the MBs by forming a double-stranded DNA (dsDNA) with S-DNA. A hairpin DNA (HP) labelled with Cy3 and Cy5 respectively at both ends was used as a fluorescence probe. The emission peaks of Cy3 and Cy5 can appear at 562 nm and 665 nm respectively, and their fluorescence intensity ratio (F_{562}/F_{665}) was chosen as the acquisition signal. The ratiometric sensor can reduce the interference of detection environment and avoid false positive reactivity. Due to the cleavage of DNAzyme and the release of single-stranded DNA (ssDNA) in the presence of Pb^{2+}, the hairpin structure of HP was opened and the FRET between two fluorophores disappeared, resulting in the strengthened signal of Cy3 and the weakened signal of Cy5. Furthermore, the ratio F_{562}/F_{665} signal increased gradually with the increase of Pb^{2+} concentration. When the concentration of Pb^{2+} was in the range of 0.1–1000 nM, F_{562}/F_{665} had a good linear relationship with $lgC_{Pb^{2+}}$, the correlation coefficient (R^2) was 0.997, and the limit of detection (LOD) was 77 pM. The presented ratiometric fluorescence biosensor had lower LOD and wider detection range via comparing with other methods. At the same time, the sensor also obtained the satisfactory results for detection of Pb^{2+} in tap water, tea, and rice flour samples. The provided ratiometric biosensor has great potential in the monitoring of various targets.

Keywords Ratiometric fluorescence biosensor · DNAzyme · Exonuclease III · Signal amplification · Lead ion

Introduction

The fluorescence sensor has many advantages such as simple experimental operation, fast response, and high sensitivity, so it was widely applied in the target detection such as heavy metals, proteins, and small molecules in recent years [1]. Ratajczak K developed a fluorescent-switching DNA aptamer–based biosensor system for the ATP level monitoring [2]. However, the sensors with a single fluorescence signal were prone to false positive results and easily disturbed by the detection environment. There, the fluorescence resonance energy transfer (FRET) between two fluorophores can easily be designed to obtain two fluorescent signals changing at the same time [3]. Compared with the single signal fluorescence sensor, the ratiometric fluorescence sensor quantitatively determines the target through the emission ratio of two signals, which can reduce the impact of detection environment and obtain low-noise results [4]. For example, Li developed a ratiometric fluorescence aptasensor based on dual dye-labelled G-quadruplex for thallium ion (TI^+) detection [5]. The G-rich aptamer of TI^+ was modified with Cy3 and Cy5 respectively at both ends. After binding with TI^+, the structure of aptamer changed to a G-quadruplex, resulting in the decreased distance between two fluorophores and the FRET from Cy3 to Cy5.

✉ Zhiguang Suo
zg_suo@163.com

[1] College of Food Science and Technology, Henan Key Laboratory of Cereal and Oil Food Safety Inspection and Control, Henan University of Technology, Zhengzhou 450001, Henan, China

[2] Henan Province Food Inspection Research Institute, 8 Jinger Road, Zhengzhou 450008, Henan, China

To improve the selectivity of fluorescence sensor, antibodies, synthetic functional nucleic acids (FNAs), and other recognition elements were used in the construction of the sensor. FNAs have many advantages such as flexible design, high affinity, low cost, strong selectivity, and good stability, which are the ideal substitute for antibodies. Research has found that FNAs such as aptamer [6, 7] and DNAzyme [8, 9] can specifically bind to a target using different modes of action. Compared with aptamer, DNAzyme cannot only specifically recognize the target, but also release the enzyme strand of DNAzyme (E-DNA) and target to circularly participate in the reaction under certain conditions, which can improve the detectability of the sensor. Heavy metal ions are the most active cofactor of DNAzyme [10]. Memon et al. developed a DNAzyme-based colorimetric sensor for detection of Pb^{2+}, on the account of the released single-stranded DNA (ssDNA) from the substrate chain of DNAzyme (S-DNA) under the action of Pb^{2+} [11]. The adsorption of ssDNA on the surface of AuNPs can effectively prevent the aggregation and color change of AuNPs under the salt induction, resulting in the potent selectivity. The sensor still achieved good results under the potential interference of other metal ions and sample matrices. Therefore, Pb^{2+}-dependent DNAzyme can be used to specifically recognize metal ions even in complex environments.

Metal ions exist widely in the environment, but the content is very small. In recent years, Pb^{2+} pollution has become one of the most common heavy metal pollutions in food. The limit of Pb^{2+} in drinking water is only 70 nM according to the US Environmental Protection Agency (EPA) [12]. Sensors with low background signal and high signal recovery can achieve sensitive detection of Pb^{2+}. Furthermore, the magnetic materials can be easily separated from the solution through magnetic separation, which can decrease the background signal [13]. As a kind of magnetic nanomaterials, magnetic beads (MBs) have uniform particle size distribution and can quickly respond to the applied magnetic field. Further, the modification of functional groups in MB surface makes it widely used [14]. Chen et al. successfully fabricated an Au-SiO_2@Fe_3O_4 magnetic nanomaterial, which can be combined with more DNAzyme systems for reaction due to the large specific surface area [15]. Therefore, MBs can be used to remove the unreacted DNAzyme from the sensor for a low background signal by magnetic separation process.

In order to improve the sensitivity of the fluorescence sensor, some signal amplification strategies were usually used such as nanomaterials and enzymes. Exonuclease III (Exo III) as an enzyme can hydrolyze the double-stranded DNA (dsDNA) from the flush or concave ends of 3′ to 5′ ends [16]. Ning designed an Exo III–assisted double-cycle fluorescence sensor for Hg^{2+} detection with a low detection limit of picomolar level [17], showing that the signal amplification strategy of Exo III in the sensor had a good effect.

Inspired by these studies, based on the FRET between Cy3 fluorescent donor and Cy5 fluorescent receptor, a low-noise ratiometric fluorescence biosensor MBs@S-DNA/E-DNA/Pb^{2+}/HP/Exo III was developed to detect Pb^{2+}. The DNAzyme structure was modified on the surface of MBs firstly, and it will be cut to form three chains under the action of Pb^{2+}. The dropped E-DNA can combine with a new S-DNA to produce the cyclic reaction, and the released ssDNA can open the HP, resulting in the disappearance of FRET between Cy3 and Cy5 labelled at both ends of HP. Here, the signal of Cy3 increased and the signal of Cy5 decreased, resulting in an increased F_{562}/F_{665}. By adding Exo III, the opened hairpin was hydrolyzed, and the falling ssDNA will open a new HP to form a cycle. In this paper, Pb^{2+}-dependent DNAzyme was chosen as the specific recognition element of Pb^{2+} to improve the selectivity of the sensor. In addition, MBs were used to reduce background signal, and DNAzyme and Exo III–assisted double signal amplification was used as the signal amplification strategy to improve the sensitivity of the sensor.

Experimental sections

Materials and chemicals

The oligonucleotides used in this paper were all synthesized by Shanghai Sangon Biotech Co., Ltd., and purified by HPLC. The sequences are as follows: substrate strand of DNAzyme (S-DNA): 5′-GGG GGG GGG GTG AGT GCT TCC ACT AT rA GGA AGA GAT GAA AAA A-$(CH_2)_6$-bio-3′; enzyme strand of DNAzyme (E-DNA): 5′-CAT CTC TTC TCC GAG CCG GTC GAA ATA GTG GAA GCA C-3′; and hairpin DNA (HP): 5′-Cy3-TGA GTG CGA AGC ACT CAC CCC CCC CCC-Cy5-3′. Tris (hydroxymethyl) aminomethane was purchased from Shanghai Shanpu Chemical Co., Ltd., ethylenediaminetetraacetic acid (EDTA) was purchased from Luoyang Chemical Reagent Factory, Tween-20 was purchased from Guangzhou Saiguo Biotechnology Co., Ltd., Exo III was purchased from Beijing Baori Doctor Physical Technology Co., Ltd., and the streptavidin-coated magnetic beads (MBs) were purchased from Suzhou Beaver Biology Co., Ltd. Buffer I (pH 7.5, 10 mM Tris, 1.04 M NaCl, 4 mM EDTA, and 500 μL Tween-20 in 1000 mL ultrapure water) and 50 mM Tris–HCl buffer (pH 7.4, 50 mM Tris, 0.2 M NaCl, and 1 mM EDTA) were used in this paper.

The construction of ratiometric fluorescence biosensor

The ratiometric fluorescence biosensor MBs@S-DNA/E-DNA/Pb^{2+}/HP/Exo III was prepared according to the

following procedures. Here, the S-DNA and E-DNA were all diluented with buffer I to maintain the dispersion of MBs during the reaction process. Firstly, 5 μL 10 mg/mL MBs were added into a 200-μL EP tube after mixing with a vortex oscillator and washed three times with 50 μL buffer I. Thereafter, 10 μL 1 μM S-DNA and 10 μL buffer I were added to the tube, and incubated in 37 °C water bath thermostatic oscillator for 1 h. The mixture was magnetic separated and washed three times with buffer I. Subsequently, 10 μL 0.5 μM E-DNA and 10 μL buffer I were added into the mixture and incubated at 37 °C for 2 h. The mixture was magnetic separated and washed three times with buffer I again.

Then, 35 μL 50 nM Pb^{2+} solution was added and incubated at 37 °C for 30 min. The supernatant was left after magnetic separation. Subsequently, 5 U Exo III and 10 μL 1 μM HP diluented with 50 mM Tris–HCl buffer were added into the supernatant and incubated at 37 °C for 1 h. The mixture was inactivated at 75 °C for 20 min and slowly reduced to room temperature in turn. Finally, the mixture was replenished to 200 μL using 50 mM Tris–HCl buffer. The fluorescence emission spectra were measured at 512-nm excitation wavelength under the conditions of 750-V voltage and 10-nm excitation and emission slit width using a G9800A fluorescence spectrophotometer (Henan Yinuojiasheng Instrument Equipment Co., Ltd.).

Application of the ratiometric fluorescence biosensor in real samples

To further study the practicality of the ratiometric fluorescence biosensor, Pb^{2+} detection was performed in tap water, tea, and rice flour. The rice flour was a certified reference material. The tea was digested by microwave, and tap water was directly used for detection of Pb^{2+}. First, 0.5 g tea, 8 mL nitric acid, and 2 mL hydrogen peroxide were added into the digestion tank. Then, the digestion tank was placed in the microwave digestion oven. The digestion parameters were set as follows: 180 °C reaction temperature, 400-psi pressure, 12-min heating time, and 15-min holding time. After digestion reaction, the digestion tank was moved to the 160 °C electric heating plate to drive out the acid in the solution. Then, the digestion tank was cooled at room temperature. Finally, the digestion solution was diluted to 10 mL with ultrapure water in a volumetric flask and mixed well for future use. The real samples were detected using the standard addition recovery method. The added scalars of Pb^{2+} were 0.5, 10, and 1000 nM. Under the optimal conditions of the MBs@S-DNA/E-DNA/Pb^{2+}/HP/Exo III sensor, the fluorescence emission spectra of the real samples were scanned, and the Pb^{2+} was determined according to the standard curve. Each sample was measured three times and averaged.

Results and discussion

Design principle of the MBs@S-DNA/E-DNA/Pb^{2+}/HP/Exo III ratiometric fluorescence biosensor

The ratiometric fluorescence biosensor was designed using Cy3 and Cy5 simultaneously as signal indicators based on DNAzyme and exonuclease III–assisted cascade signal amplification. S-DNA was immobilized on MBs by the affinity interaction between biotin on S-DNA and streptavidin on the surface of MBs, and then the E-DNA was combined with S-DNA through partial base complementary pairing to form DNAzyme. The detection principle of the MBs@S-DNA/E-DNA/Pb^{2+}/HP/Exo III sensor is shown in Scheme 1A. The DNAzyme will not be activated in the absence of Pb^{2+}. The ratiometric fluorescence biosensor will not be triggered. Thus, the hairpin structure labelled with Cy3 and Cy5 dyes at both ends will maintain stable when adding into the biosensor. Because the distance between Cy3 and Cy5 was 10 bases, an effective and stable FRET system occurred between Cy3 and Cy5, resulting in two fluorescence emission peaks at 562 nm and 665 nm, respectively [18].

S-DNA was cleaved at the modified RNA adenine base (rA) cleavage site in the presence of Pb^{2+}. Thus, the DNAzyme structure will not exist stably under the influence of the number of base coordination, and release the Pb^{2+}, E-DNA, and a single-stranded DNA (ssDNA) (Scheme 1B). The released E-DNA can combine with a new S-DNA to release more ssDNA with the help of Pb^{2+} until the S-DNA is depleted. Here, the circulation of E-DNA can obtain more released ssDNA to participate in the next reaction, which was the step 1 signal amplification. After magnetic separation, the released ssDNA in the supernatant can partially complement the HP and open the hairpin structure to form a dsDNA. After Exo III was introduced, HP contained in dsDNA can be digested into single nucleotide from the 3′ flat end, and the ssDNA contained in dsDNA was released into the solution. Hence, the distance between Cy3 and Cy5 increased and the FRET between them was eliminated which led to the fluorescence weakening of Cy5 and the enhancing of Cy3 [19]. At the same time, the released ssDNA can hybridize with a new HP and start the next round of cracking to repeatedly enhance the change of two fluorescence signals, which was the step 2 signal amplification. The fluorescence ratio of Cy3 and Cy5 was employed as a detection signal for the determination of Pb^{2+} which effectively avoids the influence of background signal compared with the single signal fluorescence sensor.

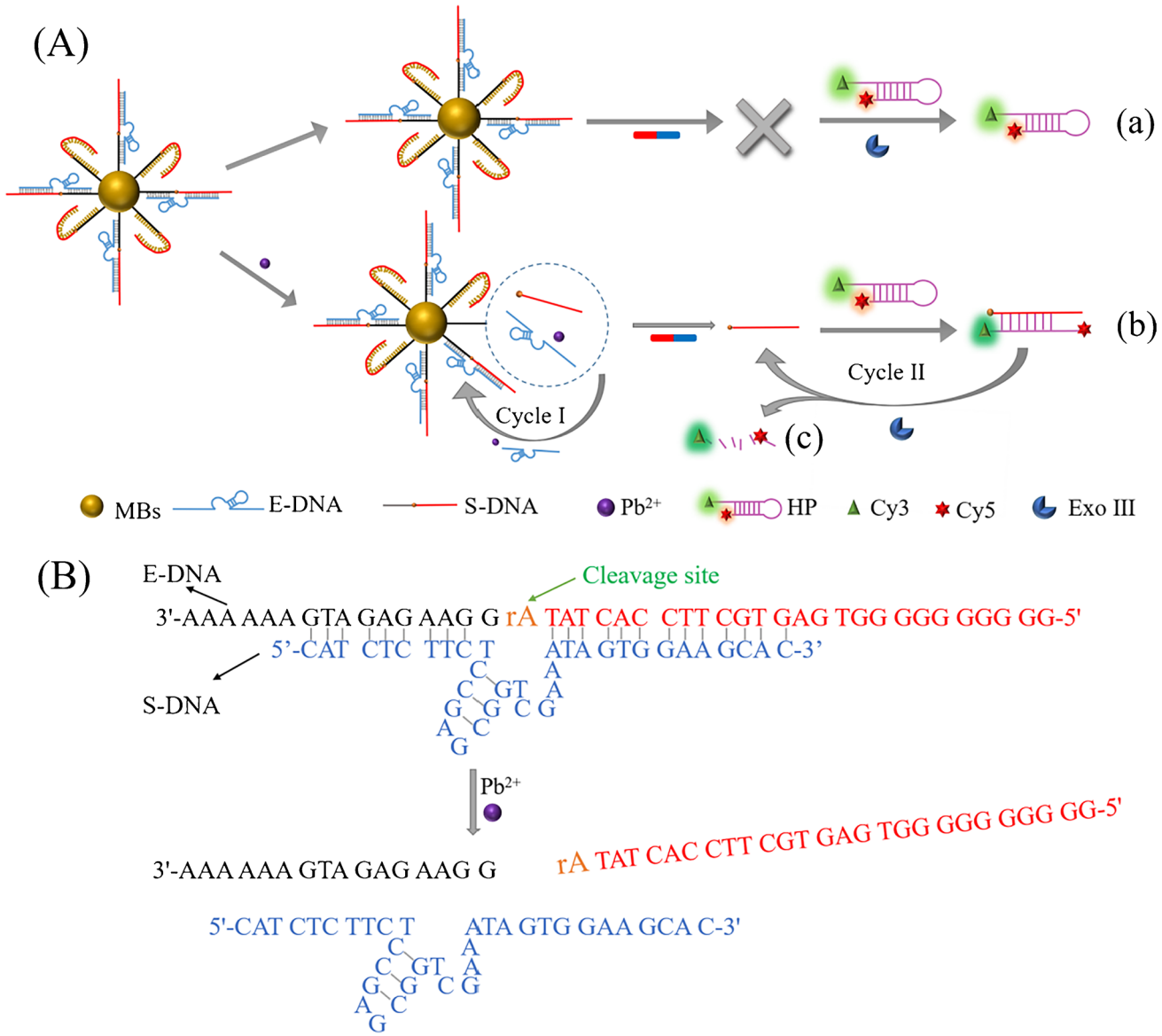

Scheme 1 (A) Schematic diagram on the fabrication of MBs@S-DNA/E-DNA/Pb^{2+}/HP/Exo III and mechanism of Pb^{2+} detection; (B) the specific structure of Pb^{2+}-dependent DNAzyme and the cleavage of S-DNA under Pb^{2+}

Feasibility analysis of the ratiometric fluorescence sensor

The prepared MBs@S-DNA/E-DNA/Pb^{2+}/HP/Exo III ratiometric fluorescence sensor was analyzed in the absence and presence of 50 nM Pb^{2+}. As shown in Fig. 1, the ratio of F_{562}/F_{665} was 1.49 in the absence of Pb^{2+} (a) and increased to 5.83 in the presence of Pb^{2+} (b). The ratio F_{562}/F_{665} increased 2.9 times compared to without Pb^{2+}, indicating the feasibility of this ratiometric fluorescence biosensor. Here, the S-DNA was cut by Pb^{2+} and released ssDNA that can combine with HP to form dsDNA. With the opening of the hairpin structure, the distance between Cy3 and Cy5 will be increased resulting in the FRET elimination between them. Then, the ratio F_{562}/F_{665} was increased to 9.72 in the presence of 50 nM Pb^{2+} and 5 U Exo III which increased 0.7 times compared with when only presence of Pb^{2+} (c). This improving signal was contributed to the enzyme digestion cyclic signal amplification strategy of Exo III. These results demonstrated the ratiometric fluorescence biosensor based on DNAzyme

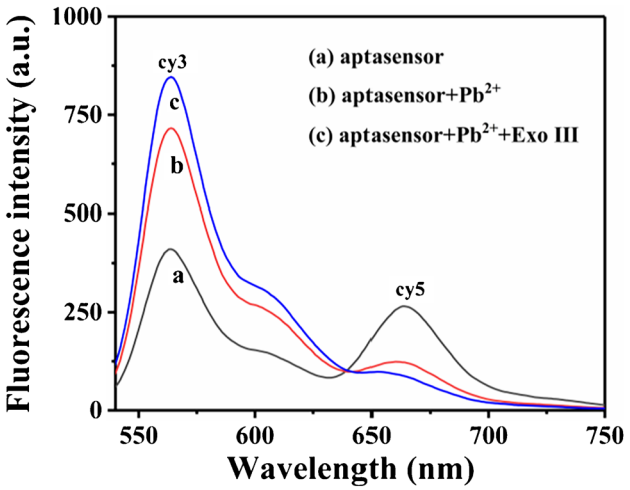

Fig. 1 The fluorescence spectra at different preparation stages. (a) MBs@S-DNA/E-DNA/HP; (b) MBs@S-DNA/E-DNA/Pb^{2+}/HP; (c) MBs@S-DNA/E-DNA/Pb^{2+}/HP/Exo III [experimental conditions: 5 μL MBs, 1 μM S-DNA, 0.5 μM E-DNA, 2-h fabrication time of sensor, 50 nM Pb^{2+}, 30-min incubation time of Pb^{2+}, and 5 U Exo III]

and Exo III–assisted cascade signal amplification can sensitively detect Pb^{2+}.

Optimization of the experimental parameters

In order to obtain the best performance of the MBs@S-DNA/E-DNA/Pb^{2+}/HP/Exo III ratiometric fluorescence biosensor, experimental parameters such as the dosage of MBs, the ratio of E-DNA to S-DNA, the fabrication time of sensor, the incubation time of Pb^{2+}, and the dosage of Exo III were optimized. Here, the experimental parameters were optimized by changing one condition at a time while keeping others unchanged. As shown in Figure S1B (see Electronic Supplementary Material), the F_{562}/F_{665} of the ratiometric fluorescence sensor gradually increased with the increasing MBs, because more DNAzyme modified in the MBs can obtain more ssDNA to involve in the reaction. When the dosage of MBs reached 5 μL, the F_{562}/F_{665} obtained the maximum value. However, the F_{562}/F_{665} decreased when dosage of MBs was higher than 5 μL on the account of the excessive MBs will agglomerate and degrade the sensor performance [20]. Therefore, 5 μL was chosen the optimum dosage of MBs. In addition, at a certain concentration of S-DNA, the F_{562}/F_{665} increased with the augment of E-DNA dosage and reached the highest value at the 0.5 of the dosage ratio of E-DNA to S-DNA. At the 0.5 of dosage ratio, the cycle reaction of E-DNA can complete the cleavage of quantitative S-DNA [21]. And, the F_{562}/F_{665} tended to be flat when the dosage ratio was over 0.5 (see Electronic Supplementary Material Figure S1D). Thus, the optimal ratio of E-DNA to S-DNA was selected as 0.5. After that, the fabrication time of sensor was respectively set at 0.5, 1, 1.5, 2, 2.5, and 3 h to obtain the optimal condition. Figure S2B (see Electronic Supplementary Material) demonstrates the influence of the sensor fabrication time on the response signal in the presence of 50 nM Pb^{2+}. Obviously, the F_{562}/F_{665} value monotonously increased at the incubation time from 0.5 to 3 h. After incubation for 2 h, the value of F_{562}/F_{665} reached to the stable. So the fabrication time of sensor was set as 2 h.

Subsequently, the incubation time of Pb^{2+} was optimized. With the prolongation of Pb^{2+} incubation time, the signal response F_{562}/F_{665} increased in the range of 5–30 min and tended to be stable, so the incubation time of Pb^{2+} was set as 30 min in the next experiment (Fig. 2B). For the excellent signal amplification, the concentration of Exo III was optimized. The F_{562}/F_{665} increased rapidly with the increase of Exo III when the dosage of Exo III was less than 5 U which profits from the potent hydrolysis efficiency of Exo III. The reaction will be saturated in the 5 U Exo III due to the limited concentration of HP (see Electronic Supplementary Material Figure S2D). Therefore, the optimal dosage of Exo III was 5 U. There, a ratiometric fluorescence biosensor was employed for the detection of Pb^{2+}.

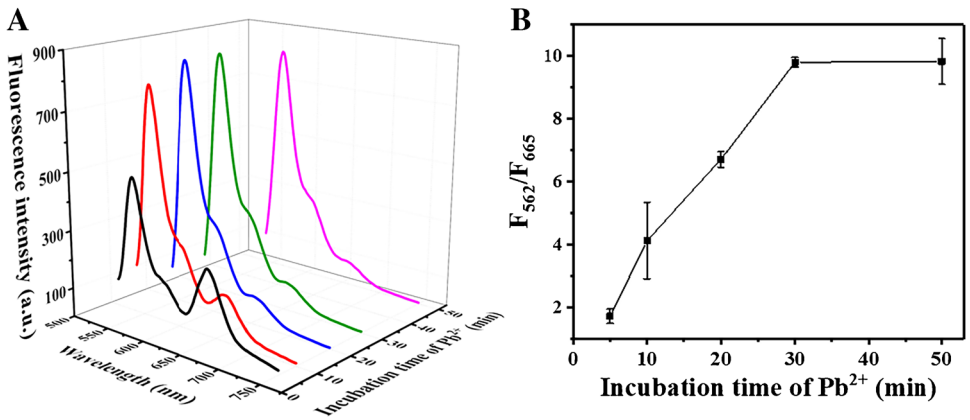

Fig. 2 Optimization of detection condition incubation time of Pb^{2+}. (A) The fluorescence spectra with different incubation times of Pb^{2+}; (B) the fluorescence intensities with different incubation times of Pb^{2+} [experimental conditions: 5 μL MBs, 1 μM S-DNA, 0.5 μM E-DNA, 2-h fabrication time of sensor, 50 nM Pb^{2+}, and 5 U Exo III]

Detection of Pb^{2+}

In recent years, the discharge of factory wastewater has been increasing with the gradual industrialization of life and production, causing serious pollution to water resources. As one of the common heavy metals, Pb^{2+} has the strongest toxicity and the widest distribution, which is abundant in the harmful substances of factory wastewater. When Pb^{2+} entered and enriched into the organisms through biological chain, it will seriously damage the immune system and nervous system, causing various diseases such as anemia, arrhythmia, and renal failure, which greatly threatens the human health [22]. Especially for infants, the enrichment of Pb^{2+} in vivo cannot only affect intelligence and development, but also leave lifelong disability [23]. Here, Pb^{2+} with various concentrations was determined using the established low-noise ratiometric fluorescence biosensor.

Under the optimal experimental conditions, F_{562}/F_{665} was measured by analyzing Pb^{2+} solution with different concentrations (Fig. 3A). It can be seen from the spectra that with the increase of Pb^{2+}, the emission peak at 562 nm increased but the peak at 665 nm decreased. The ratio F_{562}/F_{665} increased rapidly with the concentration of Pb^{2+} ranging from 0.1 to 1000 nM and tended to be flat with the further increase of Pb^{2+}. A good linear relationship was obtained between F_{562}/F_{665} and the logarithm of Pb^{2+} (Fig. 3B). The linear regression equation was $y = 3.06\lg C + 32.71$ ($R^2 = 0.997$). The LOD was calculated to be 77 pM, and the limit of quantitation (LOQ) was 258 pM according to the International Union of Pure and Applied Chemistry. The results indicated the prepared MBs@S-DNA/E-DNA/Pb^{2+}/HP/Exo III ratiometric fluorescence biosensor had good signal response and low LOD for Pb^{2+} detection. Each data was tested three times.

There, six identical sensors were prepared for 50 nM Pb^{2+} detection. The relative standard deviation (RSD) was 4.8%, indicating the good reproducibility of the ratiometric fluorescence biosensor (see Electronic Supplementary Material Figure S3A). Similarly, 50 nM Pb^{2+} was measured six times using the same sensor, and the RSD was 2% as shown in Figure S3B (see Electronic Supplementary Material), which shows that the sensor prepared in this paper had good repeatability.

To verify the selectivity, the ratio F_{562}/F_{665} responses were recorded toward different metal ions. Under the same experimental conditions, 50 nM Pb^{2+}, 5 μM interference ions such as Zn^{2+}, Hg^{2+}, Mg^{2+}, Cu^{2+}, Fe^{3+}, Mn^{2+}, $C_O{}^{2+}$, Ba^{2+}, Cd^{2+}, and K^+, and the mixture of Pb^{2+} with all interference ions were detected. As shown in Fig. 4, a high F_{562}/F_{665} value was measured in the presence of Pb^{2+} even if it coexisted with interfering ions. However, the F_{562}/F_{665} has no obvious change compared with blank sample only in the presence of interfering ions. These results showed that other metal ions cannot affect the detection performance of the sensor, indicating the excellent selectivity of the prepared ratiometric fluorescence biosensor.

To highlight the superiority of the proposed ratiometric fluorescence biosensor, a comparison is summarized in Table 1, which exhibited that the constructed MBs@S-DNA/E-DNA/Pb^{2+}/HP/Exo III sensor had lower detection limit compared with other methods for Pb^{2+} detection. The result shows that the double-cycle signal amplification strategy designed in this paper can effectively improve the detectability and reduce the detection limit of the sensor. Thus, the

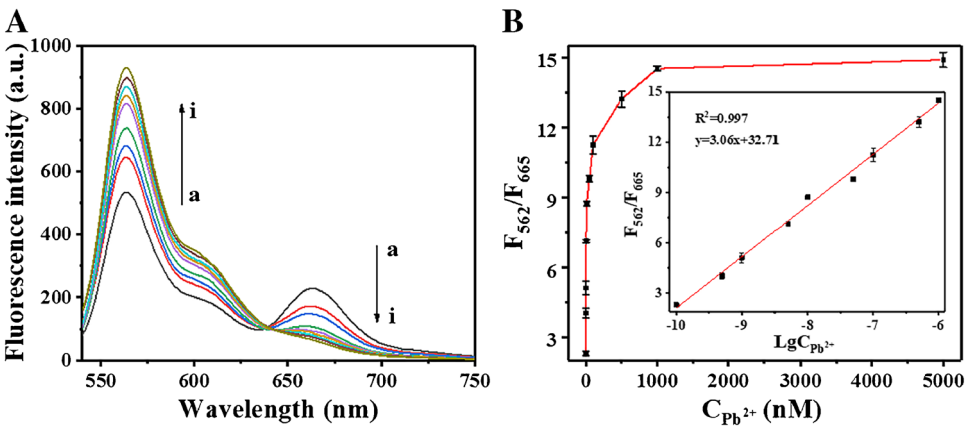

Fig. 3 (A) The fluorescence spectra of the prepared biosensor after incubation with different concentrations of Pb^{2+}: 0.1, 0.5, 1, 5, 10, 50, 100, 500, and 1000 nM; (B) the fluorescence signal of the prepared biosensor to different concentrations of Pb^{2+}: 0.1, 0.5, 1, 5, 10, 50, 100, 500, 1000, and 5000 nM. Inset: linear relationship between F_{562}/F_{665} and lg ($C_{Pb}{}^{2+}$). The concentrations of Pb^{2+}: 0.1–1000 nM [experimental conditions: 5 μL MBs, 1 μM S-DNA, 0.5 μM E-DNA, 2-h fabrication time of sensor, 30-min incubation time of Pb^{2+}, and 5 U Exo III]

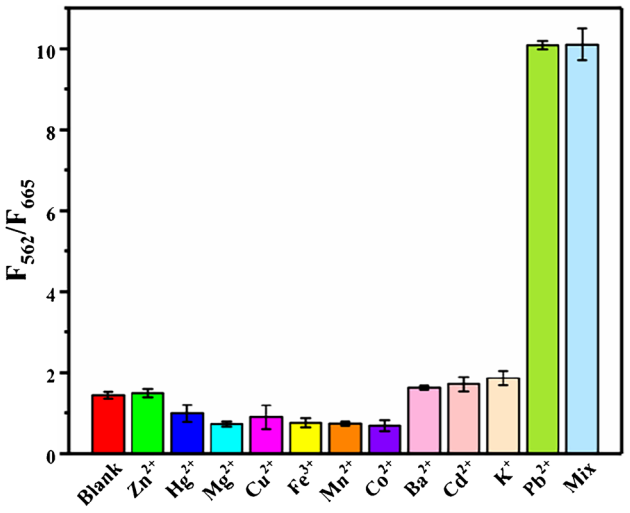

Fig. 4 The selectivity of the developed biosensor for Pb^{2+} (50 nM) compared with blank samples and other interfering ions (5 μM) [experimental conditions: 5 μL MBs, 1 μM S-DNA, 0.5 μM E-DNA, 2-h fabrication time of sensor, 30-min incubation time, and 5 U Exo III]

Table 1 Comparison with other published methods for Pb^{2+} detection

Methods	Linear range (nM)	LOD (nM)	Ref
Graphite furnace atomic absorption spectrometry	-	1	[24]
Electrochemistry	5–1000	1	[25]
Electrochemistry	100–50,000	55	[26]
Photoelectrochemical	1–10,000	0.34	[27]
Electrochemiluminescence	1–1000	1	[28]
Colorimetry	2.58–18	0.77	[29]
Fluorescence	100–1000	3.6	[30]
Fluorescence	20–1000	1	[31]
Fluorescence	0–50	4.1	[32]
Fluorescence	0.1–1000	0.077	This work

ratiometric fluorescence biosensor has potential application for sensitive detection of Pb^{2+}.

Detection of real samples

To verify the accuracy and reliability of the prepared ratiometric fluorescence biosensor in the real samples, tap water, tea, and rice flour samples were determined by the standard addition method. The added scalars of Pb^{2+} were 0.5, 10, and 1000 nM respectively. As shown in Table 2, the recoveries were in the range of 92.7–111.8% for tap water, 94.5–101.3% for tea, and 103.9–119.6% for rice flour, respectively, and their RSD was all less than 15%. The rice flour was a standard sample measured by the graphite furnace atomic absorption spectrophotometric (GFAAS) method, and the content of Pb^{2+} was 0.463 nM. According to the *t*-test method, the calculated value of *t* was 3.866, which was less than the 4.303 of $t_{(0.95,n=3)}$. The results showed that the prepared ratiometric fluorescence biosensor had a certain accuracy, and the confidence reached 95%, indicating the sensor had a strong practical application potential.

Conclusion

Based on the FRET effect between Cy3 fluorescent donor and Cy5 fluorescent receptor, a ratiometric fluorescence biosensor was developed for the detection of Pb^{2+} in food. FRET between Cy3 and Cy5 can obtain two changed fluorescence signals only through the change of the distance between them without modifying the fluorescence quenching group. The strategy can eliminate the impact of the detection environment. Here, Pb^{2+}-dependent DNAzyme can ensure the selectivity of the sensor. In addition, a double-cycle signal amplification was effectively induced by DNAzyme and Exo III, which can ensure the selectivity of the sensor. The signal was firstly amplified through the cycle of E-DNA

Table 2 The analytical results obtained from real samples using the as-fabricated ratiometric fluorescence biosensor ($n=3$)

Samples	Standard addition (nM)	Found amount (nM)	Average recovery (%)	RSD (%)
Tap water	0.5	0.46 ± 0.04	92.7 ± 0.08	9
	10	11.18 ± 0.63	111.8 ± 0.06	5.6
	1000	1062.37 ± 26.1	106.2 ± 0.03	2.5
Tea	0	0.12 ± 0.02	-	-
	0.5	0.61 ± 0.06	99.1 ± 0.11	11.3
	10	10.25 ± 0.62	101.3 ± 0.06	6.1
	1000	945.22 ± 56.08	94.5 ± 0.06	5.9
Rice flour	0	0.51 ± 0.02	-	-
	0.5	1.11 ± 0.07	119.6 ± 0.14	11.3
	10	11.85 ± 1.06	113.3 ± 0.11	9.4
	1000	1039.38 ± 37.9	103.9 ± 0.04	3.6

in DNAzyme, and further amplified with the ssDNA cycle triggered by the hydrolysis function of Exo III. There, the LOD of the sensitive ratiometric fluorescence biosensor was measured to be 77 pM, which was much lower than that of other detection methods. Even if it coexisted with interfering ions, Pb^{2+} can be specifically determined using the sensor. In addition, the ratiometric fluorescence biosensor had been successfully applied to the detection of Pb^{2+} in tap water, tea, and rice flour. In practice, the sensor has a strong potential to detect other targets by changing the DNAzyme sequences obtained through in vitro screening and amplification.

Supplementary Information The online version contains supplementary material available at https://doi.org/10.1007/s00216-021-03825-3.

Funding This study was funded by the Key Scientific and Technological Project of Henan Province (212102310001).

Declarations

Conflict of interest The authors declare no competing interests.

References

1. Li JY, Jin Y, Wang YQ, Zhao YL, Su HJ (2021) Detecting Pb^{2+} by a "turn-on" fluorescence sensor based on DNA functionalized magnetic nanocomposites. Nanotechnology. https://doi.org/10.1088/1361-6528/ac1dd3
2. Ratajczak K, Lukasiak A, Grel H, Dworakowska B, Jakiela S, Stobiecka M. Monitoring of dynamic ATP level changes by oligomycin-modulated ATP synthase inhibition in SW480 cancer cells using fluorescent "On-Off" switching DNA aptamer. Anal Bioanal Chem. 2019;411(26):6899–911. https://doi.org/10.1007/s00216-019-02061-0.
3. Wang QW, Fang T, Zheng J, Shi L, Shi LL, Li T. Proximity-dependent switchable ATP aptasensors utilizing a high-performance FRET reporter. ACS Appl Mater Interfaces. 2020;13(8):9359–68. https://doi.org/10.1021/acsami.0c15543.
4. Tian JY, Wei WQ, Wang JW, Ji SJ, Chen GC, Lu JS. Fluorescence resonance energy transfer aptasensor between nanoceria and graphene quantum dots for the determination of ochratoxin A. Anal Chim Acta. 2017;1000:265–72. https://doi.org/10.1016/j.aca.2017.08.018.
5. Li TT, Zhang Y, Sun XH, Zhang YJ, Wang YA, Nie ZY. Dual dye-labeled G-quadruplex aptasensor for detection of thallium (I) using ratiometric fluorescence resonance energy transfer. Talanta. 2021;233: 122508. https://doi.org/10.1016/j.talanta.2021.122508.
6. Ran GJ, Wu FM, Ni XY, Li XY, Li XS, Liu DL, Sun JX, Xie CF, Yao DS, Bai WB (2020) A novel label-free electrochemical aptasensor with one-step assembly process for rapid detection of lead (II) ions. Sens. Actuators, B. 320: 128326. https://doi.org/10.1016/j.snb.2020.128326
7. Chen HL, Li RT, Wu KY, Hu PP, Zhang Z, Huang NH, Zhang WH, Chen JX. Experimental and theoretical validations of a one-pot sequential sensing of Hg^{2+} and biothiols by a 3D Cu-based zwitterionic metalorganic framework-ScienceDirect. Talanta. 2020;210: 120596. https://doi.org/10.1016/j.talanta.2019.120596.
8. Chen XL, Wang XF, Lu Z, Luo HB, Dong L, Ji Z, Xu FL, Huo DQ, Hou CJ (2020) Ultra-sensitive detection of Pb^{2+} based on DNAzymes coupling with multi-cycle strand displacement amplification (M-SDA) and nano-graphene oxide. Sens. Actuators, B. 311: 127898. https://doi.org/10.1016/j.snb.2020.127898
9. Yan Y, Ma CB, Tang ZW, Chen MJ, Zhao H. A novel fluorescent assay based on DNAzyme-assisted detection of prostate specific antigen for signal amplification. Anal Chim Acta. 2020;1104:172–9. https://doi.org/10.1016/j.aca.2020.01.014.
10. Huang YY, Lin CY, Luo F, Qiu B, Guo LH, Lin ZY, Chen GN. Ultrasensitive and portable assay for lead (II) ions by electronic balance as a readout. ACS Sens. 2019;4(9):2465–70. https://doi.org/10.1021/acssensors.9b01085.
11. Memon AG, Zhou XH, Xing YP, Wang RY, Liu LH, Khan M, He M. Label-free colorimetric nanosensor with improved sensitivity for Pb^{2+} in water by using a truncated 8–17 DNAzyme. Front Environ Sci Eng. 2019;13(1):1–6. https://doi.org/10.1007/s11783-019-1094-7.
12. Liu YQ, Guo QS, Qu XJ, Sun QJ. Supramolecularly assembled ratiometric fluorescent sensory nanosystem for "traffic light"-type lead ion or pH sensing. ACS Appl Mater Interfaces. 2018;10(36):30662–9. https://doi.org/10.1021/acsami.8b10007.
13. Zhao ST, Xiao JX, Wang HL, Li LX, Wang K, LV JG, Zhang Z,. Rapid heavy metal sensing platform: a case of triple signal amplification strategy for the sensitive detection of serum copper. Anal Chim Acta. 2021;1181: 338908. https://doi.org/10.1016/j.aca.2021.338908.
14. Rocha-Santos TAP. Sensors and biosensors based on magnetic nanoparticles. TrAC. Trends Anal Chem. 2014;62:28–36. https://doi.org/10.1016/j.trac.2014.06.016.
15. Chen XJ, Ge LN, Guo BH, Yan M, Hao N, Xu L. Homogeneously ultrasensitive electrochemical detection of adenosine triphosphate based on multiple signal amplification strategy. Biosens Bioelectron. 2014;58:48–56. https://doi.org/10.1016/j.bios.2014.02.043.
16. Yang XY, Wang LH, Pang LD, Fu SQ, Qin X, Chen Q, Man CX, Jiang YJ. A novel fluorescent platform of DNA-stabilized silver nanoclusters based on exonuclease III amplification-assisted detection of Salmonella Typhimurium. Anal Chim Acta. 2021;1181: 338903. https://doi.org/10.1016/j.aca.2021.338903.
17. Ning Y, Hu J, Wei K, He G, Wu T, Lu F. Fluorometric determination of mercury(II) via a graphene oxide-based assay using exonuclease III-assisted signal amplification and thymidine-Hg(II)-thymidine interaction. Microchim Acta. 2019;186(4):216. https://doi.org/10.1007/s00604-019-3332-x.
18. Deng JK, Liu YQ, Lin XD, Lyu YL, Qian PC, Wang S. A ratiometric fluorescent biosensor based on cascaded amplification strategy for ultrasensitive detection of kanamycin. Sens Actuators, B. 2018;273:1495–500. https://doi.org/10.1016/j.snb.2018.07.065.
19. Deng JK, Niu XJ, Liu YQ, Wang S. A ratiometric fluorescent biosensor based on exonuclease III amplification strategy for pathogenic bacterial gene detection. Chin J Anal Chem. 2018;46(5):743–9. https://doi.org/10.11895/j.issn.0253.3820.181091.
20. Lian FN, Wang D, Yao S, Ge LR, Wang Y, Zhao YY, Zhao JB, Song XL, Zhao C, Li JH, Liu YJ, Jin MH, Xu K. A detection method of Escherichia coli O_{157}:H_7 based on immunomagnetic separation and aptamers-gold nanoparticle probe quenching Rhodamine B's fluorescence. Food Sci Biotechnol. 2021;30(8):1129–38. https://doi.org/10.1007/s10068-021-00947-3.
21. Yang YJ, Huang J, Yang XH, Quan K, Wang H, Ying L, Xie NL, Ou M, Wang KM. Aptazyme-gold nanoparticle sensor for amplified molecular probing in living cells. Anal Chem. 2016;88(11):5981–7. https://doi.org/10.1021/acs.analchem.6b00999.

22. Taiwo AM, Olukayode S, Ojekunle OZ, Oyedepo JA, Awomeso JA, Gbadebo AM (2021) The content and toxicological risk assessment of trace elemental impurities (Pb and Cr) in snacks from Ogun State, Southwestern Nigeria. Biol. Trace Elem. Res. (prepublish). https://doi.org/10.1007/S12011-021-02839-3
23. Yao WC, Gallagher DL, Gohlke JM, Dietrich AM. Children and adults are exposed to dual risks from ingestion of water and inhalation of ultrasonic humidifier particles from Pb-containing water. Sci Total Environ. 2021;791: 148248. https://doi.org/10.1016/j.scitotenv.2021.148248.
24. Cadorim HR, Schneider M, Hinz J, Luvizon F, Dias AN, Carasek E, Welz B. Effective and high-throughput analytical methodology for the determination of lead and cadmium in water samples by disposable pipette extraction coupled with high-resolution continuum source graphite furnace atomic absorption spectrometry (HR-CS GF AAS). Anal Lett. 2019;52(13):1–17. https://doi.org/10.1080/00032719.2019.1596117.
25. Yang R, Fang TF, Lu LP, Ye Q. Highly sensitive detection of Pb^{2+} based on DNAzyme/AuNPs-GO sensor by square-wave voltammetry. Chin J Anal Chem. 2021;49(2):309–17. https://doi.org/10.19756/j.issn.0253-3820.201231.
26. Xu TT, Dai HQ, Jin YC. Electrochemical sensing of lead(II) by differential pulse voltammetry using conductive polypyrrole nanoparticles. Microchim Acta. 2019;187(1):23–23. https://doi.org/10.1007/s00604-019-4027-z.
27. Cao JT, Liao XJ, Wang YL, Liu YM. A novel photoelectrochemical strategy for lead ion detection based on CdSe quantum dots cosensitized ZnO-CdS nanostructure. J Electroanal Chem. 2020;880:114828. https://doi.org/10.1016/j.jelechem.2020.114828.
28. Hao TT, Zhang CF, Lin H, Wei WT, Yang F, Wu YB, Niu LM, Kang WJ, Guo ZY. A one-step dual-mode aptasensor for subnanomolar detection of lead ions based on electrochemiluminescence and fast scan voltammetry. J Electrochem Soc. 2020;167(12): 126506. https://doi.org/10.1149/1945-7111/abaf76.
29. Yang GY, Song CL, Shi QW, Liu HW, Li SY, Liu R, Liu SM, Lv CY. Amplified colorimetric sensor for detecting radon by its daughter lead based on the free-fixed auto-assembly structure of Duplex-hemin/G-quadruplex. J Pharm Biomed Anal. 2018;159:459–65. https://doi.org/10.1016/j.jpba.2018.07.026.
30. Geng FH, Wang DD, Feng L, Li GX, Xu MT. An improved structure-switch aptamer-based fluorescent Pb^{2+} biosensor utilizing the binding induced quenching of AMT to G-quadruplex. Chem Commun. 2020;56(72):10517–20. https://doi.org/10.1039/d0cc03669b.
31. Xia JY, Xu T, Qing J, Xiong Y, Liu JJ, Gong FC. Highly sensitive sensor for lead ion based on thioflavin T-induced G-quadruplex formation. Chem Res Chin Univ. 2020;41(5):1004–9. https://doi.org/10.7503/cjcu20190689.
32. Wang Y, Lv MH, Chen ZH, Deng ZL, Liu NT, Fan JW, Zhang WX. A fluorescence resonance energy transfer probe based on DNA-modified upconversion and gold nanoparticles for detection of lead ions. Front Chem. 2020;8:238. https://doi.org/10.3389/fchem.2020.00238.